Electronic Supplementary Material (ESI)

for

Ligand Redox Controlled Amine Dehydrogenation and Imine Hemilability in Singlet Diradical Azo-aromatic Ni(II) Complexes: Characterization of the Electron Transfer Series of Azo-imine Complexes of Ni(II)

Bappaditya Goswami,[†a] Manas Khatua,[†a,c] Ambika Devi,[b] Shivali Hans,[b] Robindo Chatterjee,[b] Subhas Samanta[*b]

[a]Department of Chemical Sciences, Indian Institute of Science Education and Research Kolkata, Mohanpur, Nadia, West Bengal 741246, India

[b]Department of Chemistry, Indian Institute of Technology Jammu, Jagti, Jammu, Jammu and Kashmir 181221, India

[c]Current Affiliation: Central Instrumentation Facility, Indian Institute of Technology (IIT) Jammu, Paloura, Jammu, Jammu and Kashmir 181121, India

***Correspondence:** Dr. Subhas Samanta, subhas.samanta@iitjammu.ac.in

[†]These authors contributed equally to this work and share first authorship.

Table of Contents

Contents **page**

Tables **page**

A. Synthesis of Ligands

The ligands, **L²** and **L³** were prepared and purified according to our reported literature procedure.[1-5] Their yields and characterization data are as follows:

L²: Yield: 83%; ESI-MS m/z 317.1403 amu; IR (KBr): ν = 1501 cm^{-1} (N=N), 1627 cm^{-1} (C=N); UV-vis: ε_{240nm}, 41779 M^{-1} cm^{-1}, ε_{351}nm, 59288 M^{-1} cm^{-1}; ε_{443}nm, 863 M^{-1} cm^{-1}; ^{1}H NMR (500 MHz, $CDCl_3$) δ 8.81 (s, 1H), 8.34 (dd, *J* = 7.6, 0.9 Hz, 1H), 8.10-8.08 (m, 2H), 8.01-7.97 (m, 1H), 7.86 (dd, *J* = 7.9, 1.0 Hz, 1H), 7.43 (t, *J* = 7.6 Hz, 2H), 7.33 (d, *J* = 7.6 Hz, 2H), 7.06-7.02 (m, 3H), 3.91 (s, 3H); $^{13}C\{^{1}H\}$ NMR (500 MHz, $CDCl_3$) δ 163.27 (C), 163.22 (C), 160.25 (C), 154.34 (C-H), 150.64 (C), 146.69 (C-H), 138.83 (C-H), 129.27 (C-H), 126.92 (C-H), 125.90 (C-H), 122.34 (C-H), 121.20 (C-H), 114.84 (C-H), 114.32 (C-H), 55.63 (CH_3).

L³: Yield: 78%; ESI-MS m/z 305.1202 amu; IR (KBr): ν = 1504 cm^{-1} (N=N), 1628 cm^{-1} (C=N); UV-vis: ε_{226nm}, 50976 M^{-1} cm^{-1}, ε_{324}nm, 58050 M^{-1} cm^{-1}, ε_{461}nm, 1103 M^{-1} cm^{-1}; $^{19}F\{^{1}H\}$ NMR (500 MHz, $CDCl_3$) δ -115.29; ^{1}H NMR (500 MHz, $CDCl_3$) δ 8.79 (s, 1H), 8.36 (d, *J* = 7.6 Hz, 1H), 8.09-8.07 (m, 2H), 8.01 (t, *J* = 7.8 Hz, 1H), 7.88 (d, *J* = 7.9 Hz, 1H), 7.57-7.53 (m, 3H), 7.35-7.31 (m, 2H), 7.12 (t, *J* = 8.7 Hz, 2H); $^{13}C\{^{1}H\}$ NMR (500 MHz, $CDCl_3$) δ 162.94 (C), 160.86 (C), 159.69 (C), 154.34 (C-H), 152.19 (C), 146.52 (C-H), 138.96 (C), 132.48 (C-H), 129.18 (C-H), 123.69 (C-H), 122.80 (C-H), 116.17 (C-H), 115.99 (C-H), 115.16 (C-H).

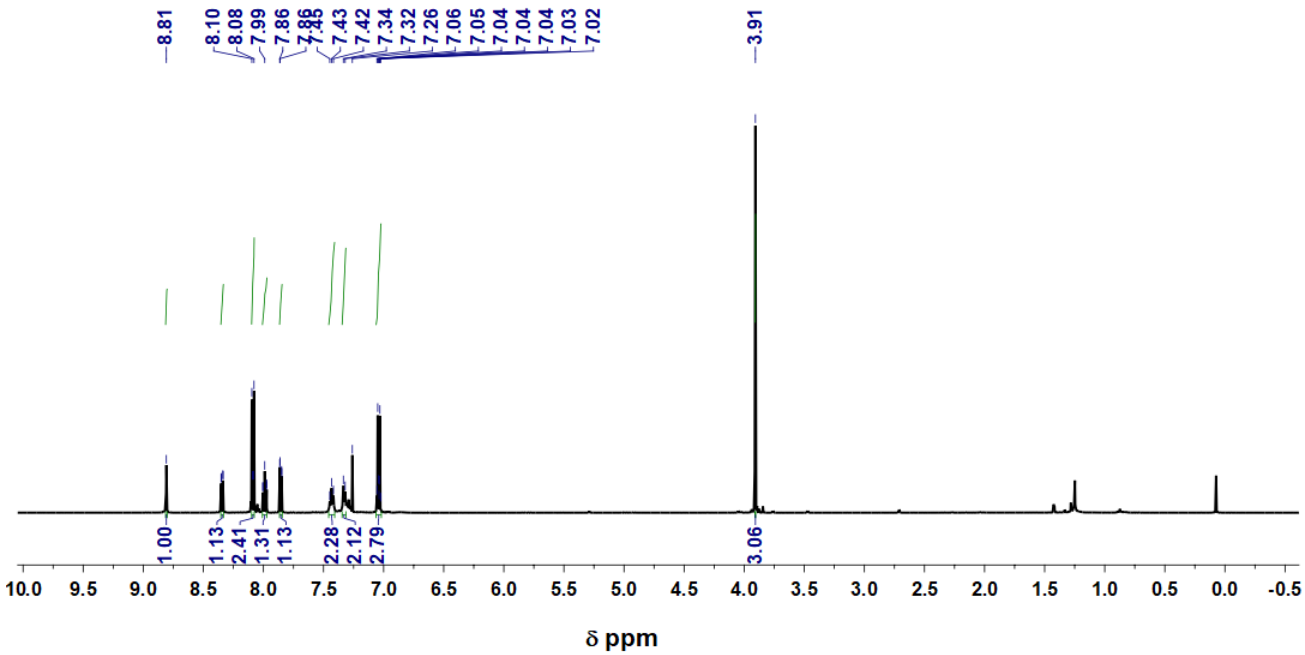

Figure S1: ^{1}H NMR spectra of ligand $\mathbf{L^2}$ in $CDCl_3$ in 500 MHz at 298K.

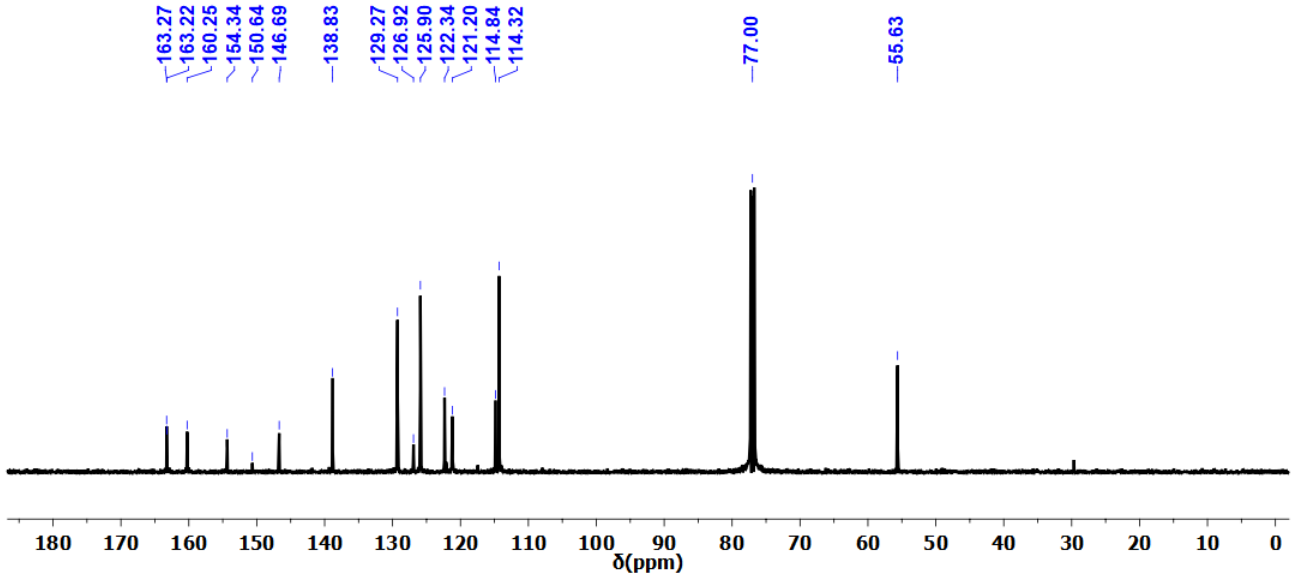

Figure S2: $^{13}C\{^{1}H\}$ NMR spectra of ligand $\mathbf{L^2}$ in $CDCl_3$ in 500 MHz at 298K.

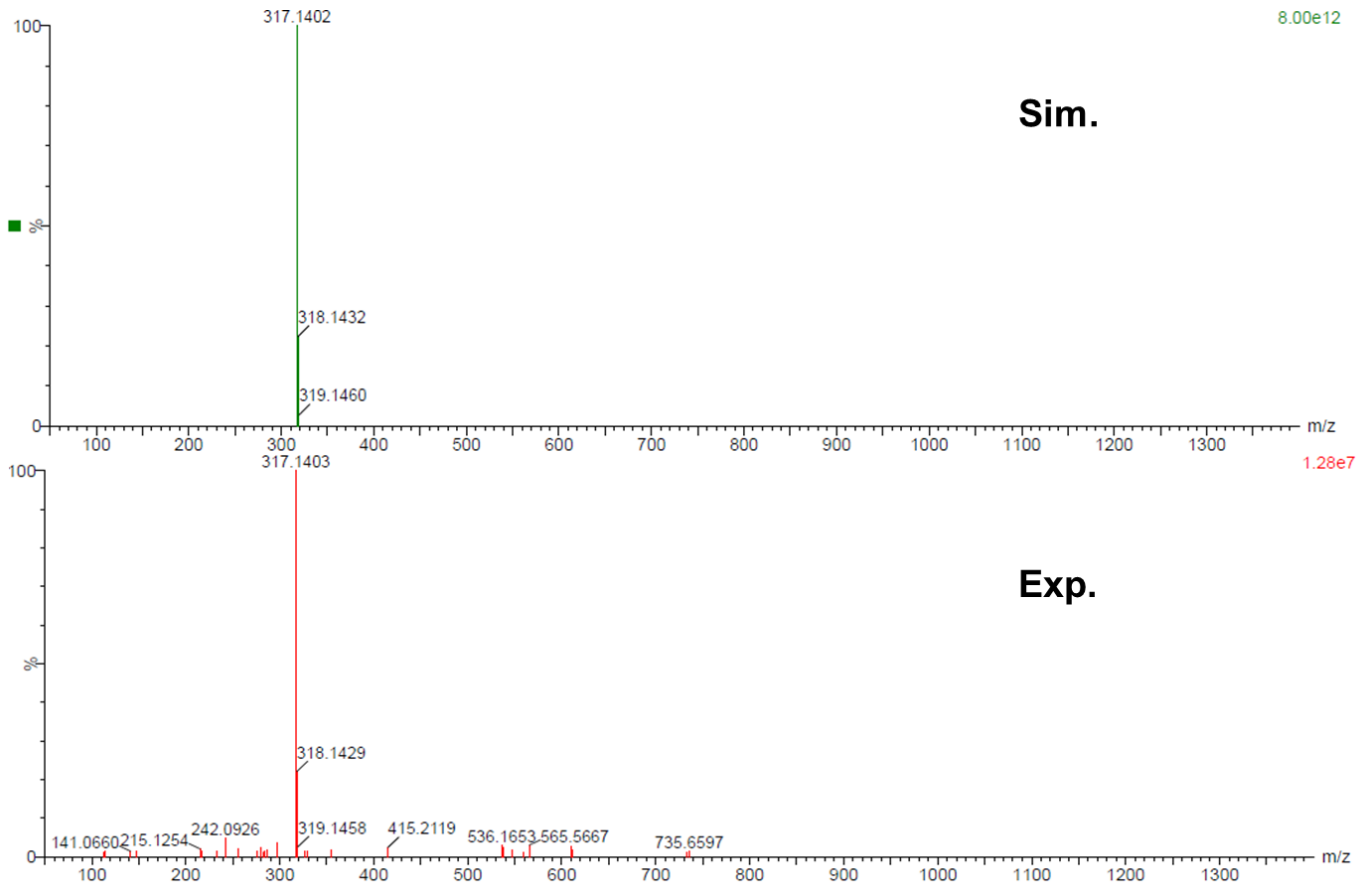

Figure S3: ESI-MS of ligand $\mathbf{L^2}$ in methanol.

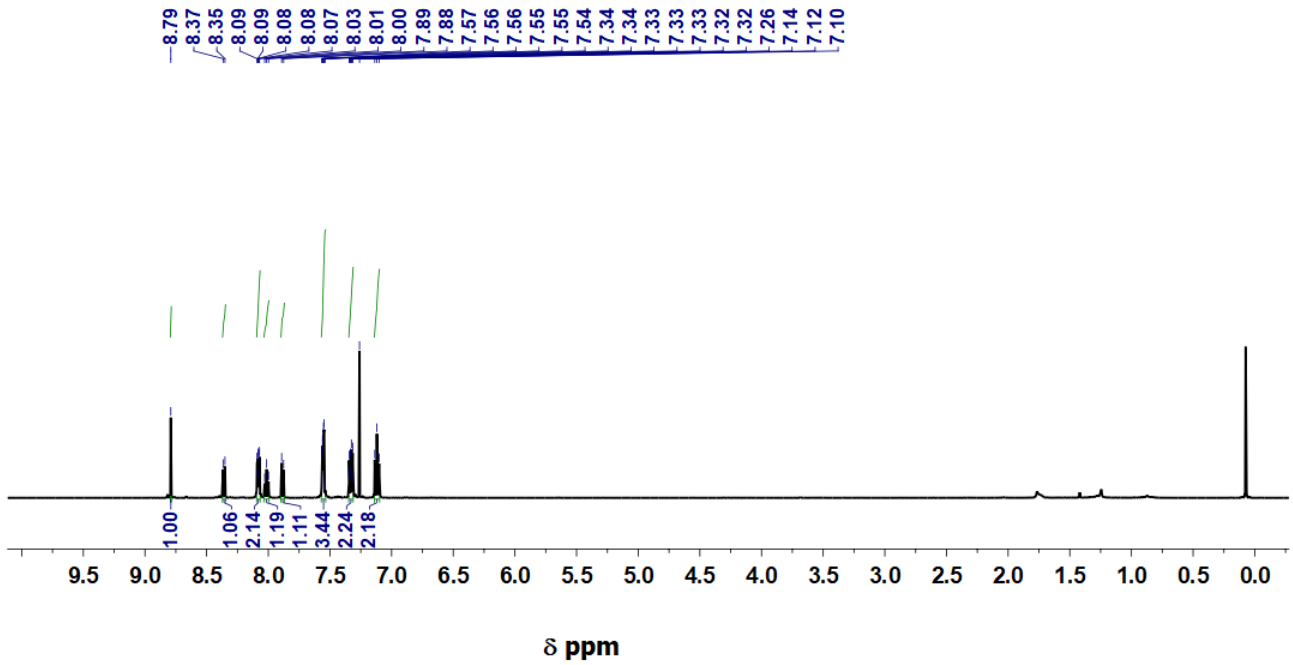

Figure S4: ^{1}H NMR spectra of ligand **L^{3}** in $CDCl_3$ in 500 MHz at 298K.

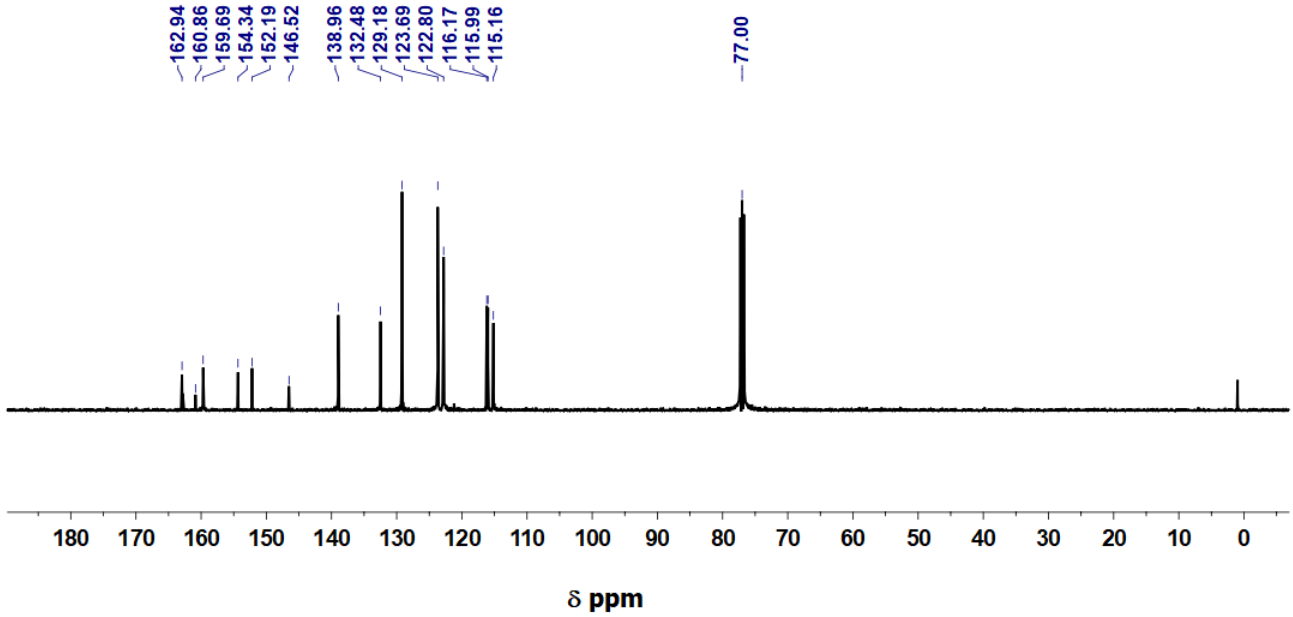

Figure S5: ^{13}C{^{1}H} NMR spectra of ligand **L^{3}** in $CDCl_3$ in 500 MHz at 298K**.**

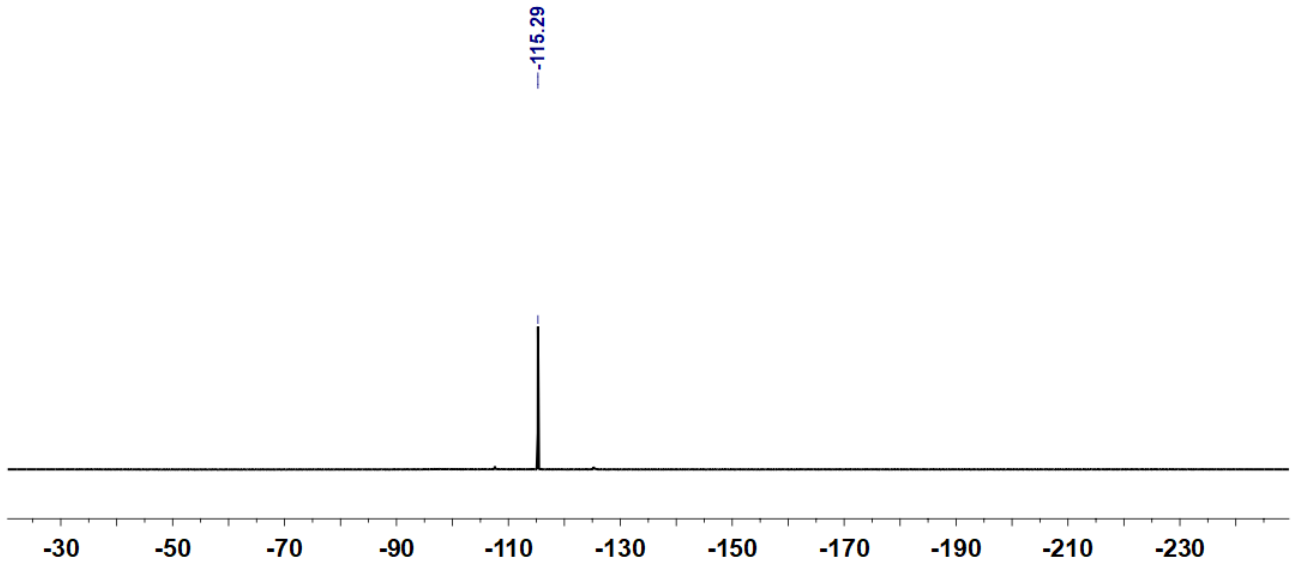

Figure S6: $^{19}F\{^{1}H\}$ NMR spectra of ligand **L³** in $CDCl_3$ in 500 MHz at 298K.

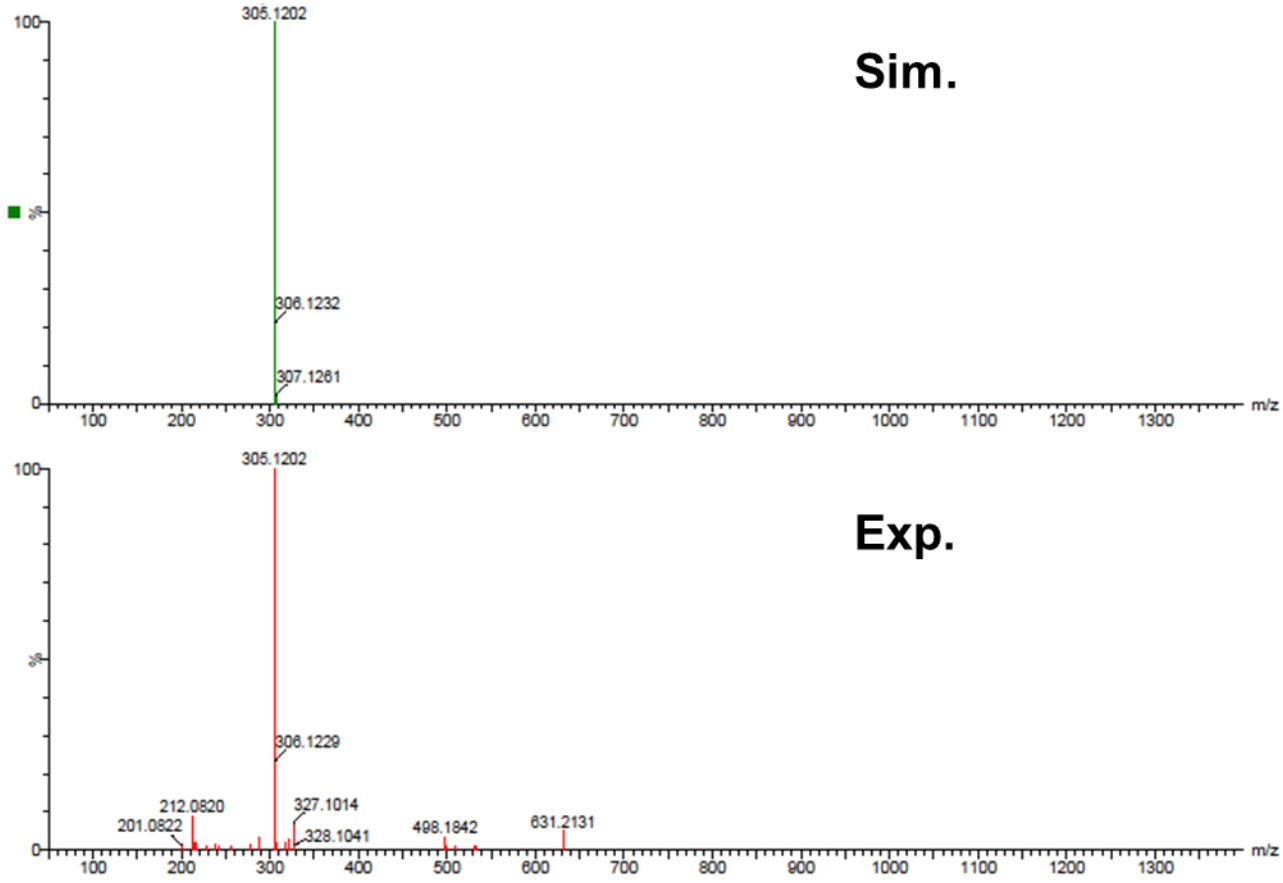

Figure S7: ESI-MS of ligand **L³** in methanol.

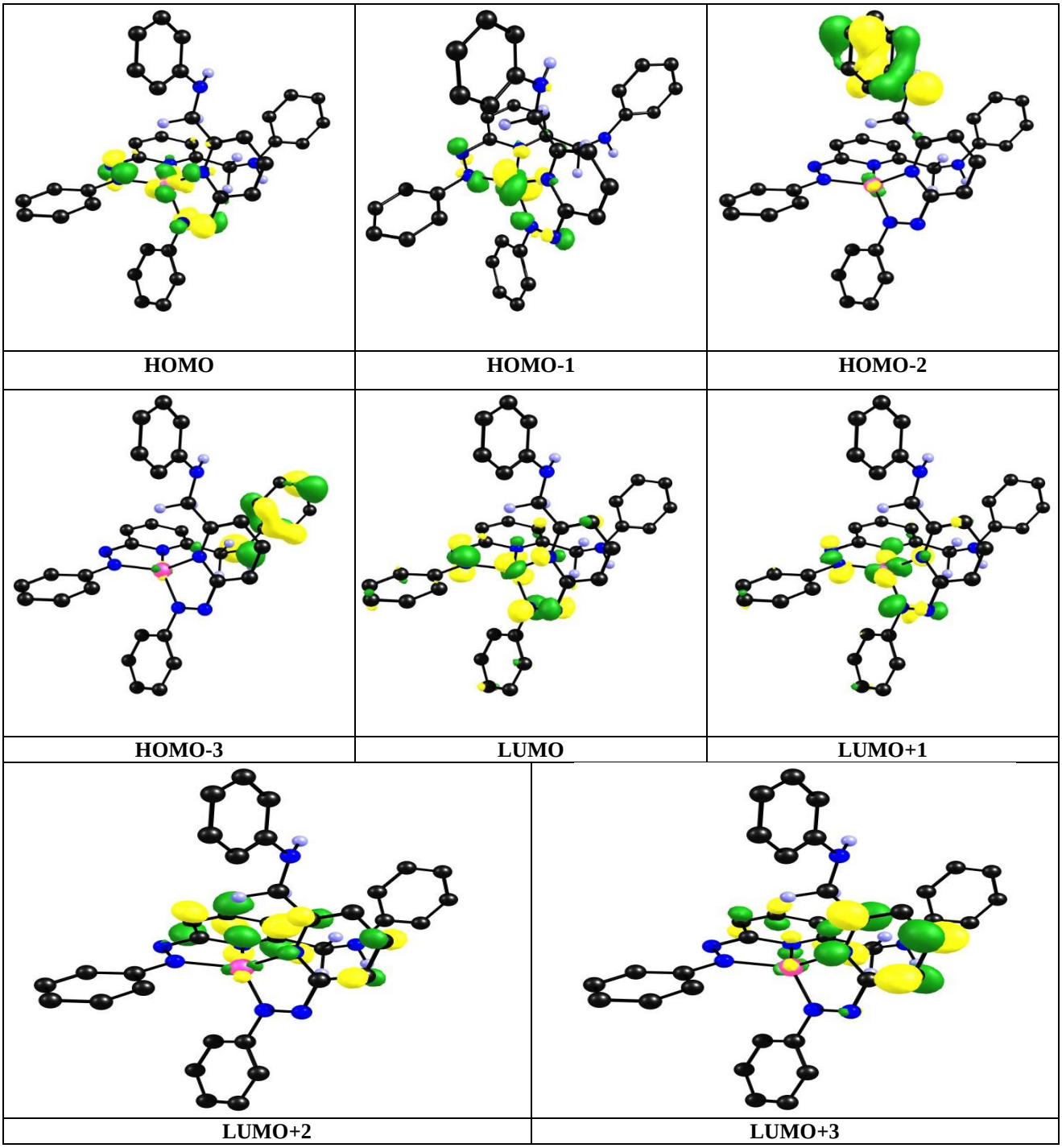

Figure S8. Molecular Orbitals of Complex **[1]** *(isosurface value= 0.06)*

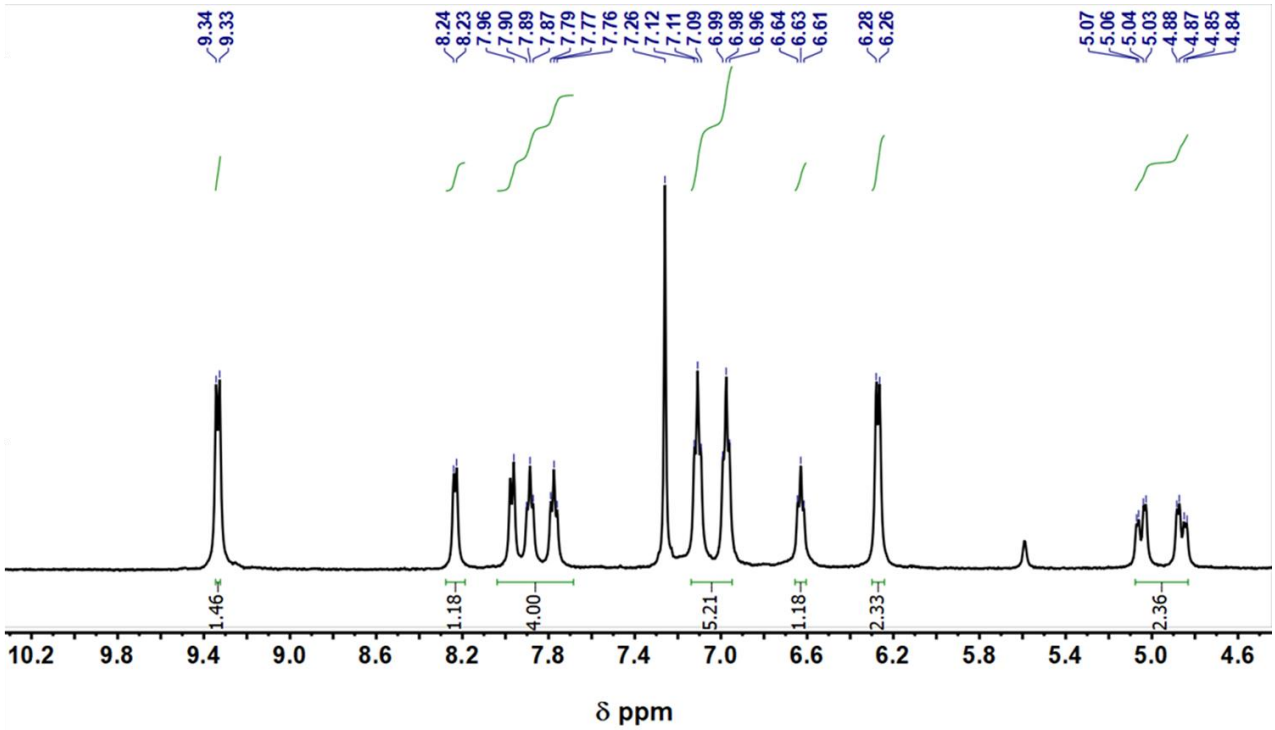

Figure S9. ^{1}H NMR spectra of complex [**1**] in $CDCl_3$ in 500 MHz at 298K.

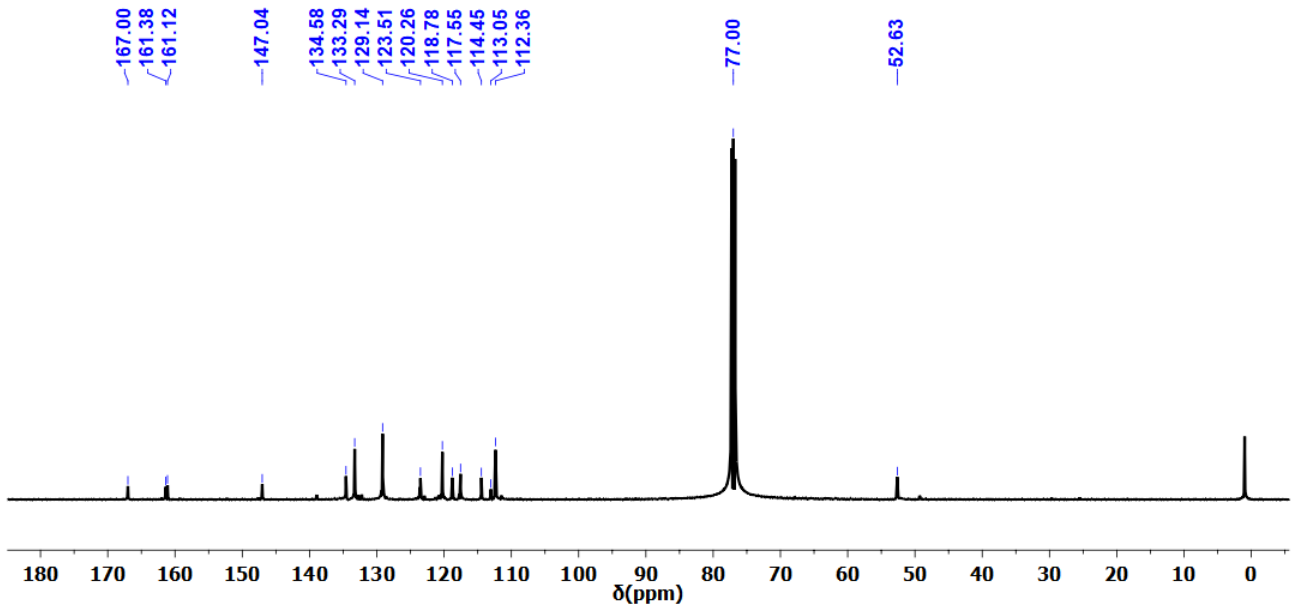

Figure S10. ^{13}C{^{1}H} NMR spectra of complex [**1**] in $CDCl_3$ in 500 MHz at 298K.

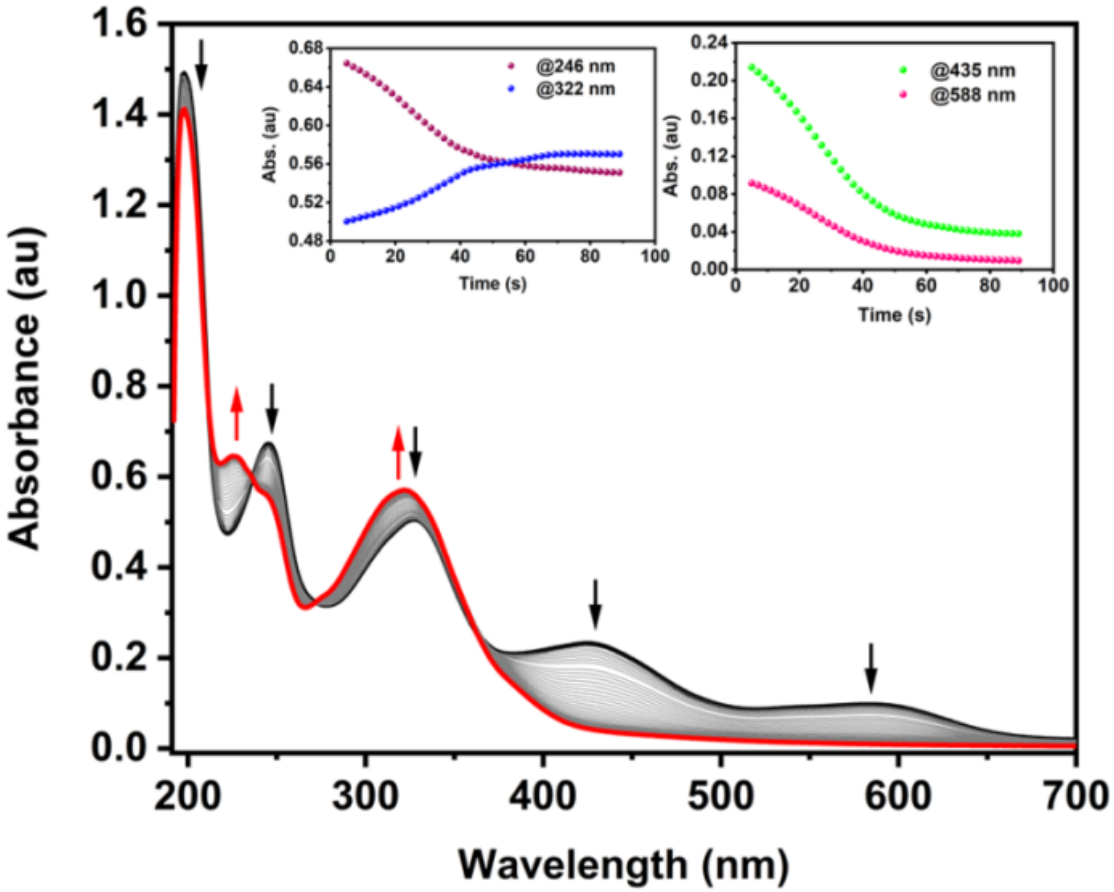

Figure S11. Time-dependent UV-vis spectrum of [**1**] in acetonitrile solution upon exposure to air at 298K.

B. Procedure for the reaction of complex [1] with O_2

In 10 mL of dry degassed acetonitrile, 100 mg (0.15 mmol) of compound **1** was dissolved in a 25 mL of Schlenk tube. Subsequently, the molecular oxygen was bubbled by a balloon over a period of 10 minutes into the solution. The colour of the reaction mixture immediately changed from dark brown to orange red. After 10 minutes of stirring at room temperature, the reaction mixture was evaporated under reduced pressure. The crude product was extracted thrice using 5 mL of diethyl ether. The combined ether solution was filtered through a cellite pad, and the filtrate was collected. The solvent was evaporated under reduced pressure and the product was characterized by ^{1}H NMR. Analysis of the product showed that 90% of **L^1** (major) and 10% of **H_2L** (minor).

Scheme S1. Reaction of the complex [**1**] with O_2

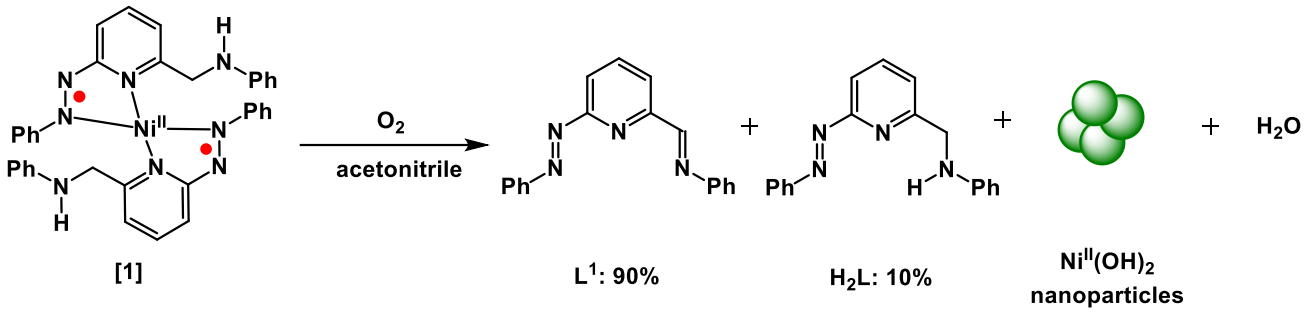

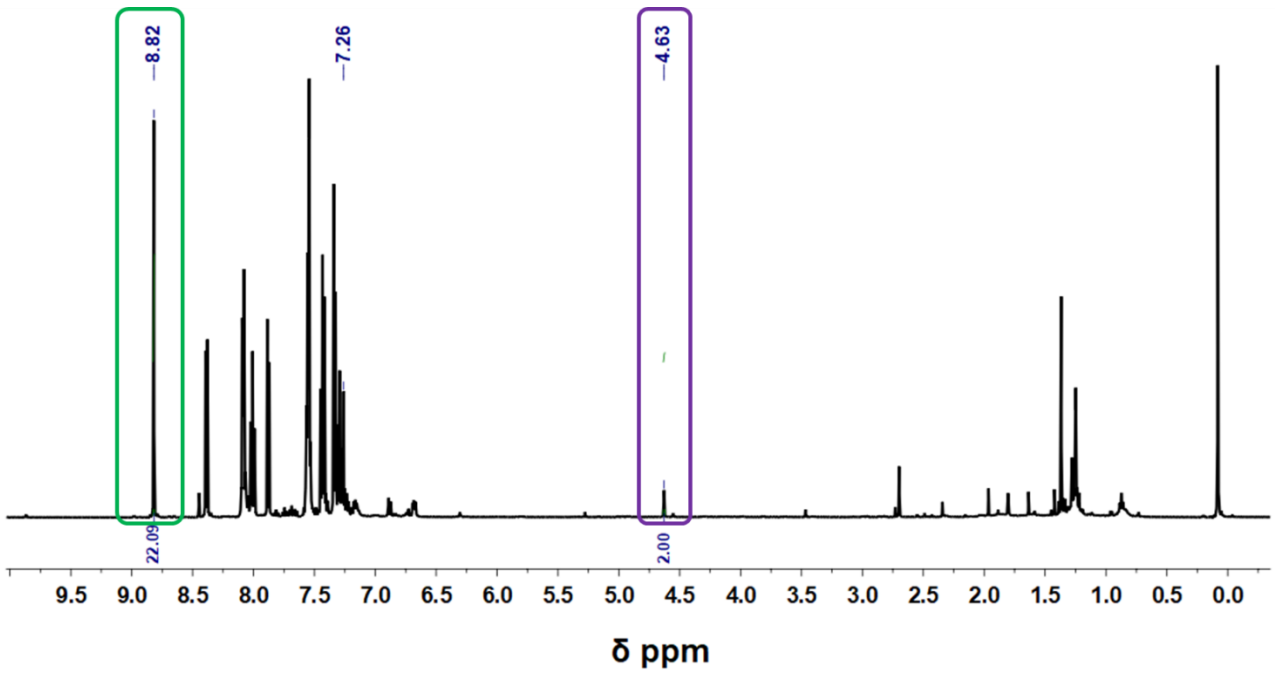

Figure S12. ^{1}H NMR of the reaction mixture of complex [**1**] upon exposure to O_2

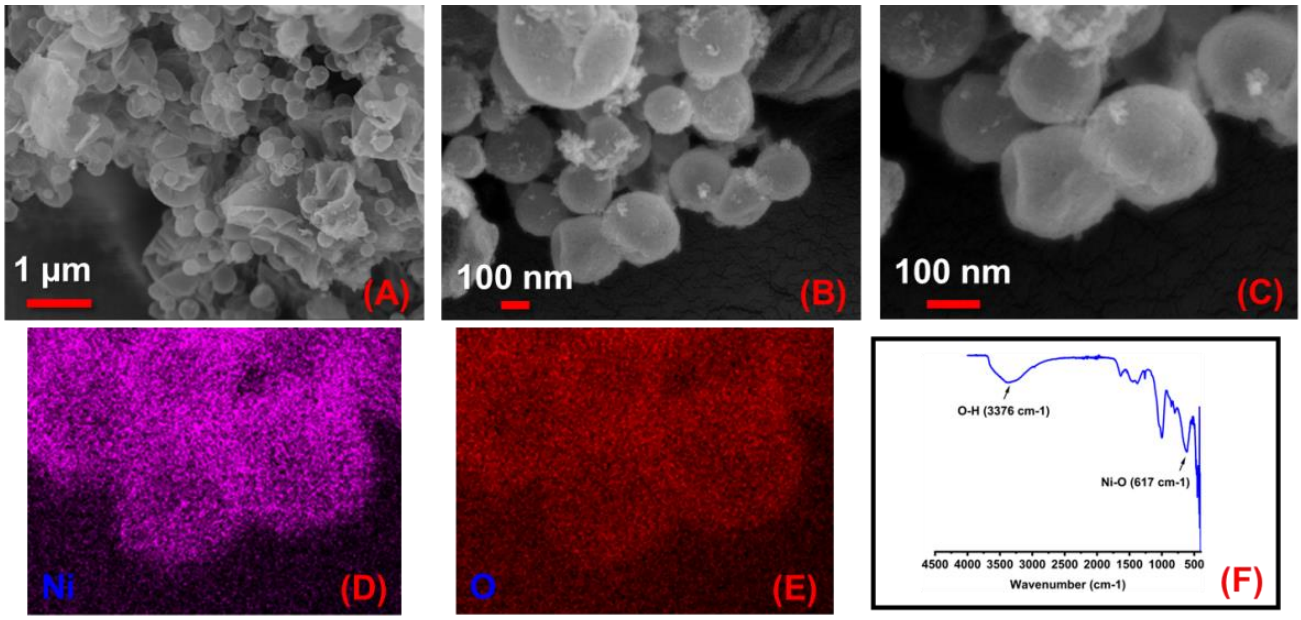

Figure S13. FESEM images (**A-C**); EDS-mapping images for different elements (**D, E**); FT-IR spectrum of $Ni(OH)_2$ (**F**).

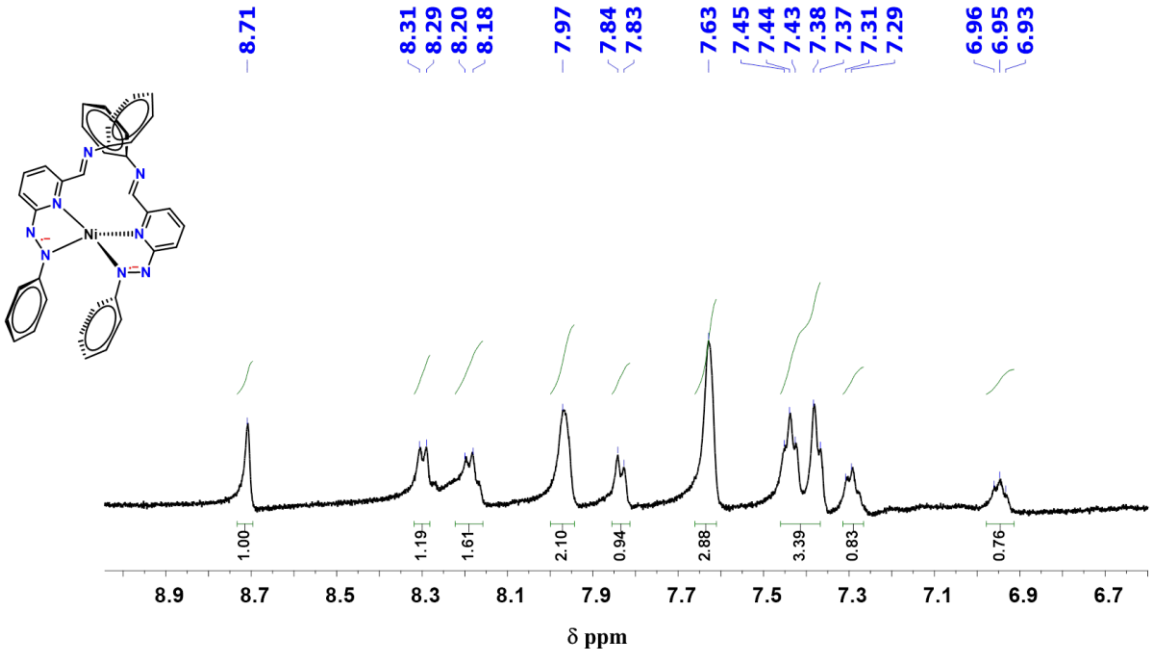

Figure S14. ^{1}H NMR spectra of complex [**2**] in DMSO-d_6 in 500 MHz at 298K.

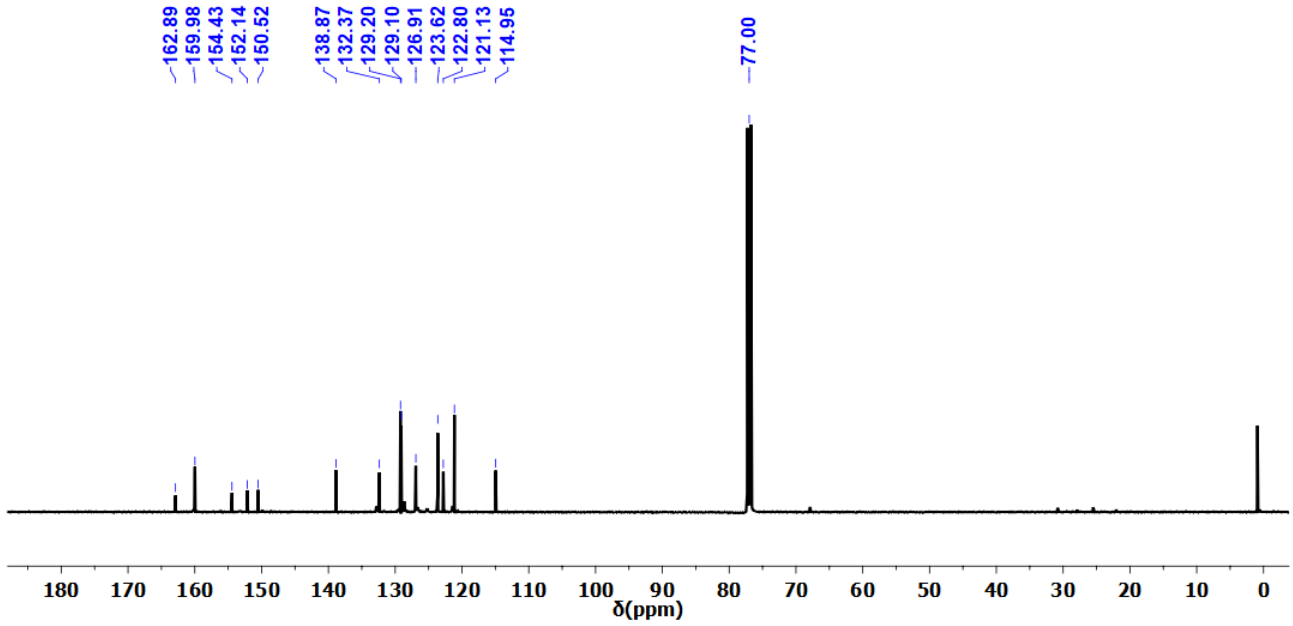

Figure S15. ^{13}C{^{1}H} NMR spectra of complex [**2**] in $CDCl_3$ in 500 MHz at 298K.

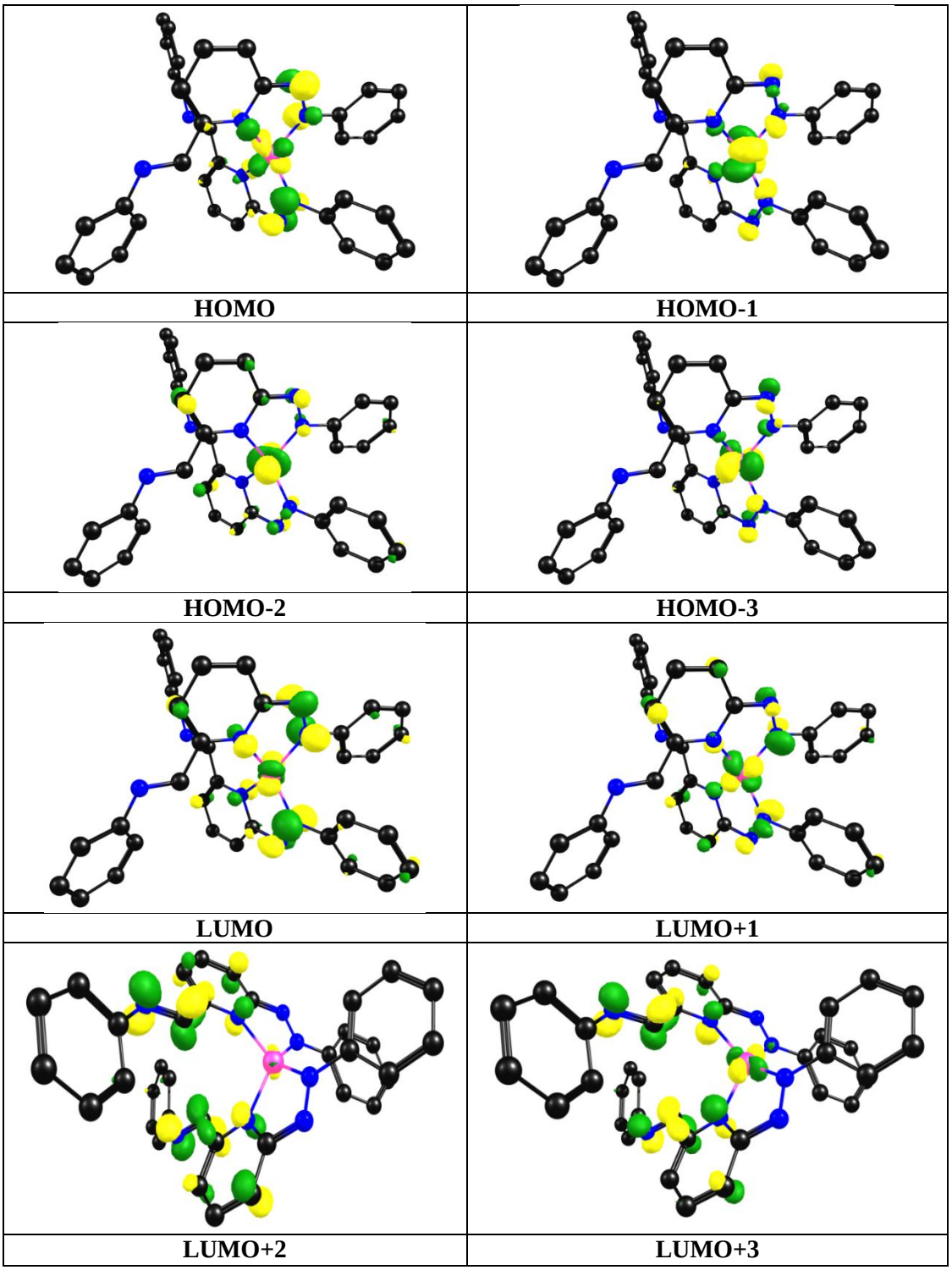

Figure S16. Molecular Orbitals of Complex **[2]** *(isosurface value= 0.06)*

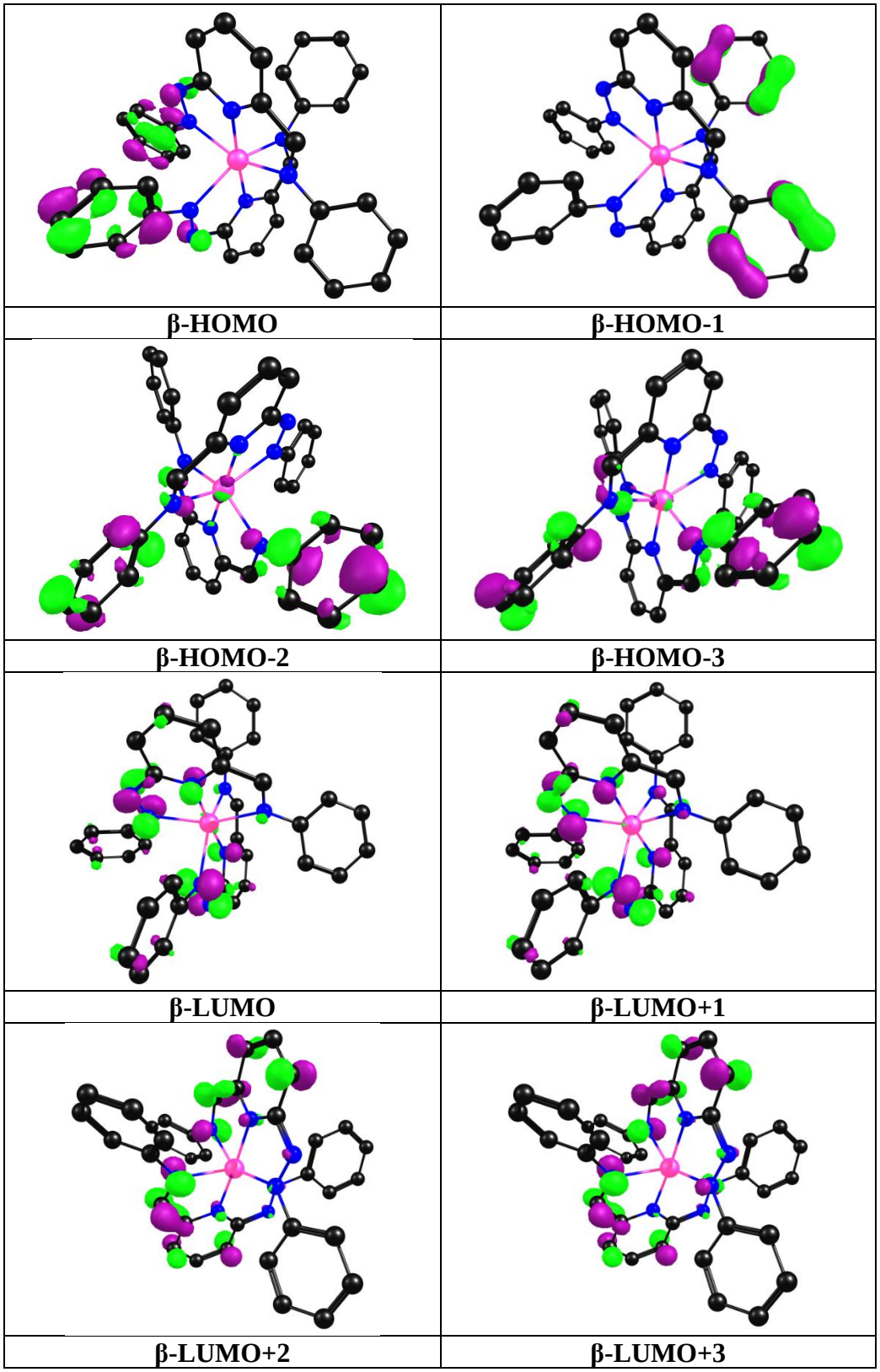

Figure S17. Molecular Orbitals of Complex **[3a](ClO_4)$_2$** *(isosurface value= 0.06)*

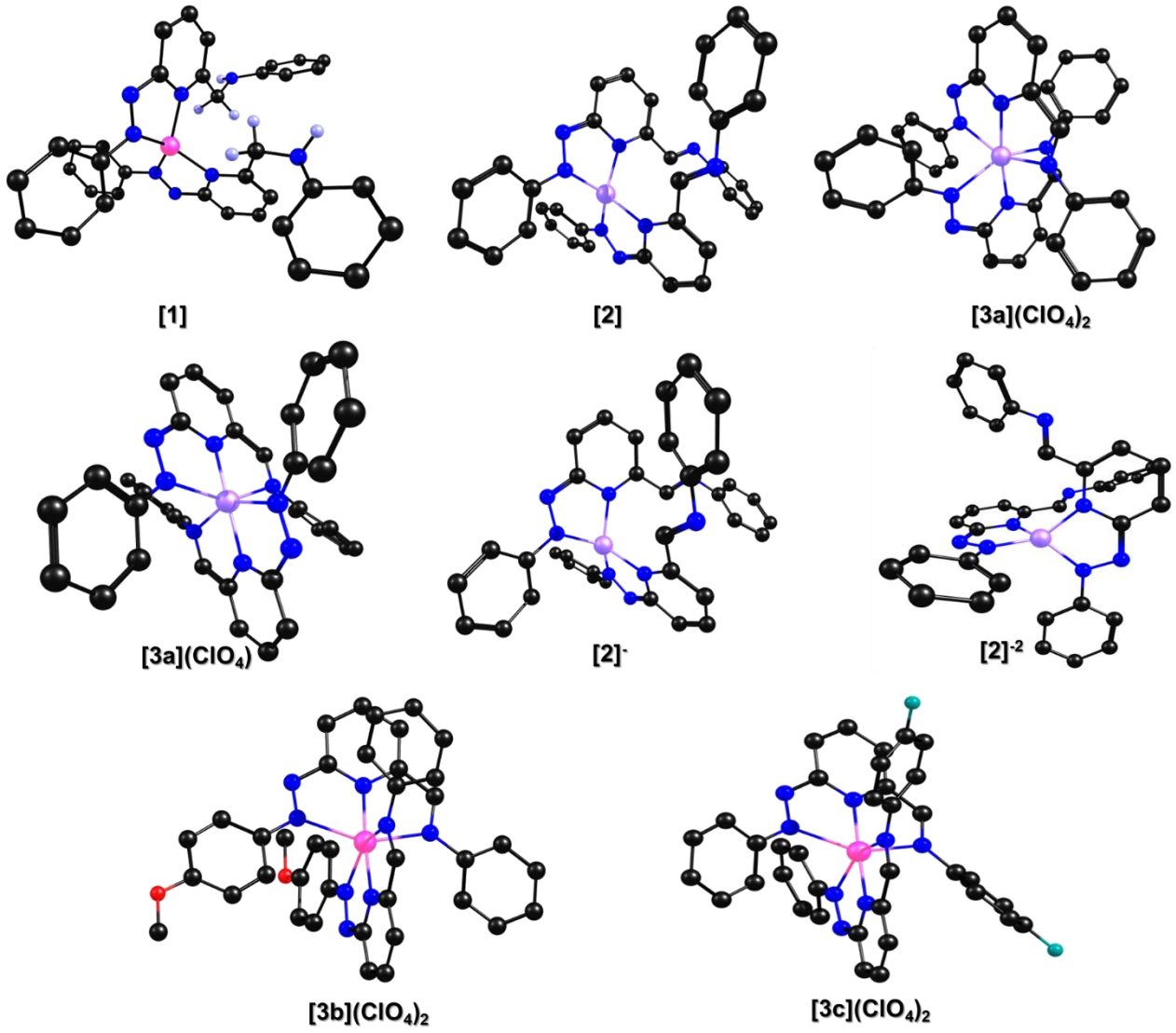

Figure S18. Optimized Structure of the complexes [**1**], [**2**], [**3a**]$(ClO_4)_2$, [**3a**](ClO_4), [**2**]$^-$, [**2**]$^{2-}$, [**3b**]$(ClO_4)_2$ and [**3c**]$(ClO_4)_2$.

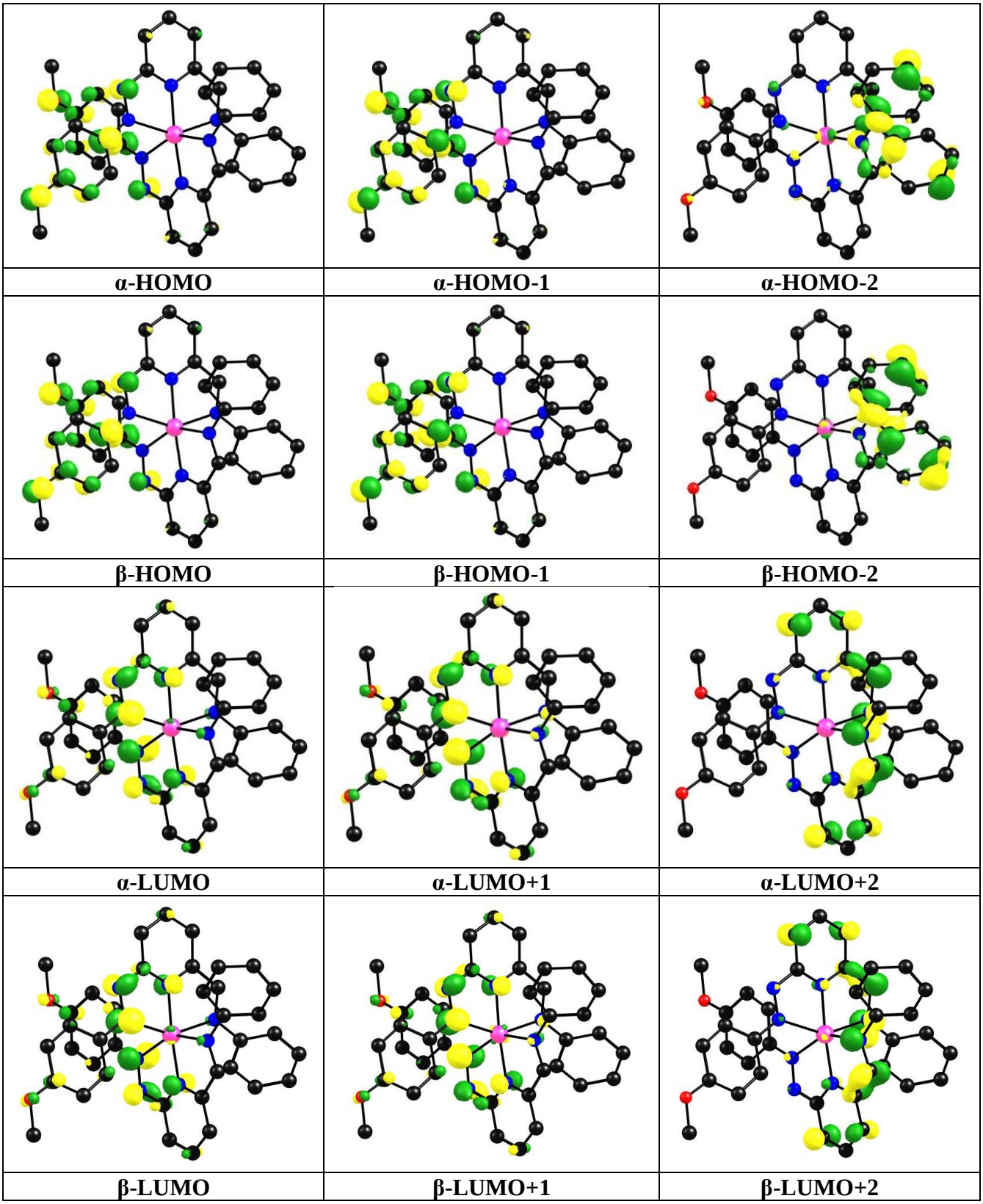

Figure S19. Molecular Orbitals of Complex **[3b](ClO$_4$)$_2$** *(isosurface value= 0.06)*

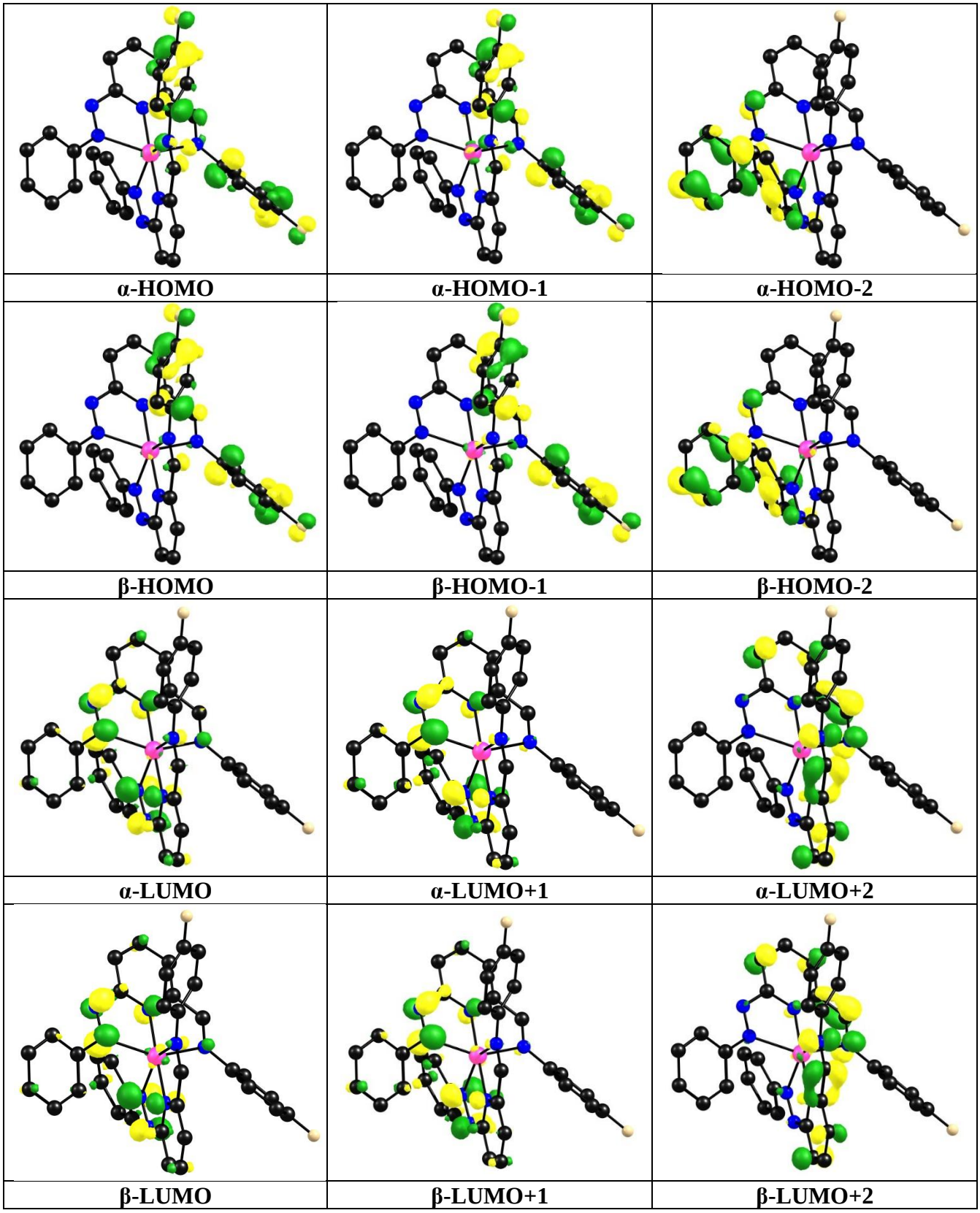

Figure S20. Molecular Orbitals of Complex **[3c](ClO$_4$)$_2$** *(isosurface value= 0.06)*

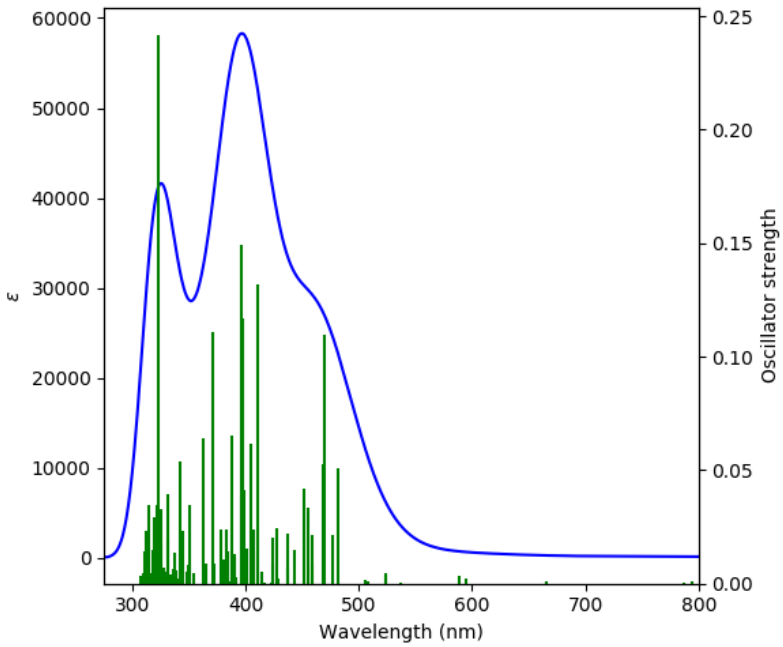

Figure S21. TDDFT Calculated absorption spectrum of the complex, [**3a**]$(ClO_4)_2$

Table S1. TDDFT calculated major excited state transitions of the complex, [**3a**]$(ClO_4)_2$ with Osc. Strength and λ_{ex}.

λ_{ex} (nm) (Exp.)[a]	λ_{ex} (nm) (Calc.)[b]	Oscillator Strength (*f*)	Major Transitions[c]
315	323.4	0.2419	H-2 (α) → L+3 (α) (20%), H-9 (β) → L+1 (β) (14%)
381	396.2	0.1495	H-6 (α) → LUMO (α) (15%), H-4 (α) → L+1 (α) (15%), H-4 (β) → L+1 (β) (32%)
549	588.3	0.0033	H-9 (α) → L+1 (α) (24%), H-8 (α) → L (α) (20%)
613	665.4	0.0008	H-2(α) → LUMO(α) (17%), H-1(α) → LUMO(α) (11%), H-2(β) → LUMO(β) (17%)

[a]Experimental wavelength in dichloromethane. [b]TD-DFT calculated wavelength of the complex, [**3a**]$(ClO_4)_2$. [c]Transitions with greater than 10% contribution are presented.

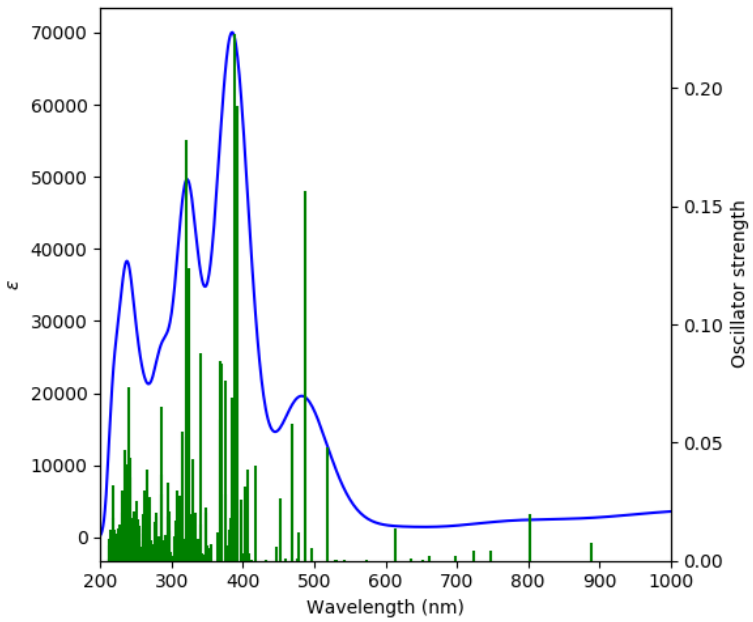

Figure S22. TDDFT Calculated absorption spectrum of the complex, [**3a**](ClO_4)

Table S2. TDDFT calculated major excited state transitions of the complex, [**3a**](ClO_4) with Osc. Strength and λ_{ex}.

λ_{ex} (nm) (Exp.)[a]	**λ_{ex} (nm) (Calc.)[b]**	**Oscillator Strength (*f*)**	**Major Transitions[c]**
316	320.6	0.2008	H-12 (α) → LUMO (α) (18%), H-13 (β) → LUMO (β) (10%), H-12 (β) → LUMO (β) (18%)
379	389.3	0.2231	H-5 (α) → LUMO (α) (16%), H-1 (β) → L+1 (β) (28%)
595	613.1	0.0138	H-3 (α) → L+1 (α) (14%), HOMO (α) → L+1 (α) (69%)

[a]Experimental wavelength in dichloromethane. [b]TD-DFT calculated wavelength of complex, [**3a**](ClO_4). [c]Transitions with greater than 10% contribution are presented.

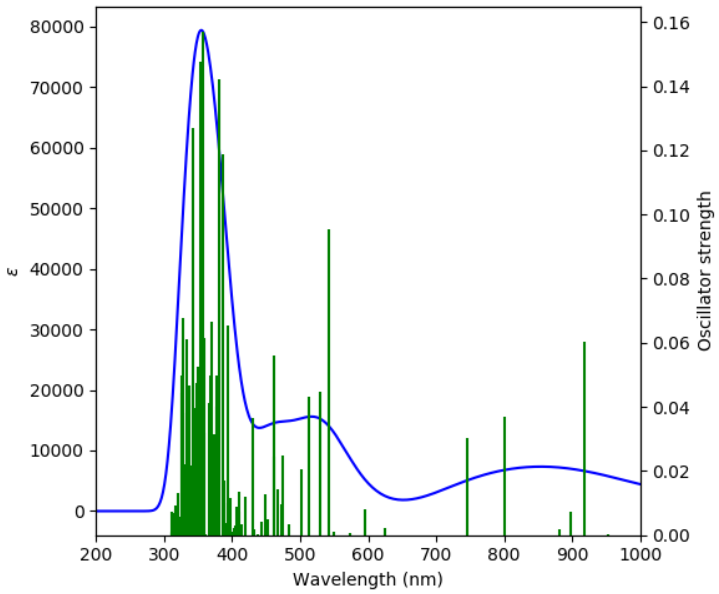

Figure S23. TDDFT Calculated absorption spectrum of the complex, [**2**]

Table S3. TDDFT calculated major excited state transitions of the complex, [**2**] with Osc. Strength and λ_{ex}.

λ_{ex} (nm) (Exp.)[a]	λ_{ex} (nm) (Calc.)[b]	Oscillator Strength (*f*)	Major Transitions[c]
315	356.9	0.1571	HOMO (β) → L+11 (β) (46%), HOMO (β) → L+12 (β) (12%)
381	386.8	0.1187	H-3 (α) → L+1 (α) (20%), H-4 (β) → LUMO (β) (23%), H-1 (β) → L+4 (β) (14%)
594	542.8	0.0955	H-3(α) → LUMO (α) (23%), H-1 (α) → LUMO (α) (42%)
890	917.6	0.0604	HOMO (α) → L+2 (α) (17%), HOMO (β) → L+1 (β) (60%)

[a]Experimental wavelength in dichloromethane. [b]TD-DFT calculated wavelength of the complex, [**2**]. [c]Transitions with greater than 10% contribution are presented.

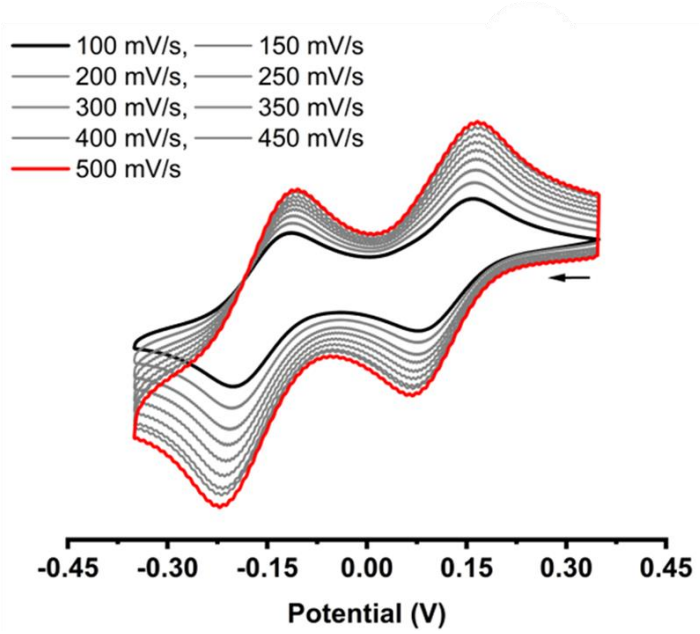

Figure S24. Cyclic voltammogram of complex **[2]** in dichloromethane solution at different scan rate.

C. References:

1. M. Khatua, B. Goswami and S. Samanta, *Dalton Trans.*, 2020, **49**, 6816-6831.

2. B. K. Barman, M. Khatua, B. Goswami, S. Samanta and R. K. Vijayaraghavan, *Chem Asian J.*, 2021, **16**, 1545−1552.

3. B. Goswami, M. Khatua and S. Samanta, *Dalton Trans.*, 2022, **51**, 1454−1463.

4. B. Goswami, M. Khatua, R. Chatterjee, Kamal and S. Samanta, *Organometallics*, 2023, **42**(15), 1854−1868.

5. Kamal, M. Khatua, S. Rani, B. Goswami and S. Samanta, *J. Org. Chem.*, 2023, **88**(9), 5827−5843.